

Anomaly Detection of Test-Time Evasion Attacks using Class-conditional Generative Adversarial Networks*

Hang Wang, David J. Miller and George Kesidis
School of EECS, Pennsylvania State University, University Park, PA, 16802, USA
{hzw81,djm25,gik2}@psu.edu

May 24, 2021

Abstract

Deep Neural Networks (DNNs) have been shown vulnerable to adversarial (Test-Time Evasion (TTE)) attacks which, by making small changes to the input, alter the DNN's decision. We propose an attack detector based on class-conditional Generative Adversarial Networks (GANs). We model the distribution of clean data conditioned on the predicted class label by an Auxiliary Classifier GAN (ACGAN). Given a test sample and its predicted class, three detection statistics are calculated using the ACGAN Generator and Discriminator. Experiments on image classification datasets under different TTE attack methods show that our method outperforms state-of-the-art detection methods. We also investigate the effectiveness of anomaly detection using different DNN layers (input features or internal-layer features) and demonstrate that anomalies are harder to detect using features closer to the DNN's output layer.

1 Introduction

In recent years, vulnerabilities of Deep Neural Networks (DNN) have attracted significant attention. It has been shown that, for a given test image to be classified, a malicious attacker can alter the image with small, often imperceptible perturbations chosen to induce the DNN to change its decision [4]. This is called a Test-Time Evasion attack (TTE) or an “adversarial sample”. It is important, both in terms of security and to increase trust in and reliability of DNN decision making, to understand TTEs and to devise defenses against them.

Several works [17][8] have shown that DNNs may overfit a training set, and thus may not generalize well on out-of-training-distribution test samples. Accordingly, various schemes have been proposed to detect such samples and/or to robustify the DNN. We categorize these methods as follows: i) adversarial training; ii) ensembles of models; and iii) anomaly detection. Adversarial training methods [13] create adversarial examples (labeled to their true class of origin) and include such supervising examples in classifier training. Adversarial training improves robustness in input-space regions close to training samples; however this is achieved with some reduction in accuracy on clean data [24]. Moreover, adversarially trained DNNs may still be vulnerable to *other* adversarial inputs. Thus, such training may not resolve the fundamental problem. Other works propose a Neural Network ensemble defense [23][6] wherein several sub-networks are trained, with decisions made by soft voting of the sub-networks. However, adversarial examples have been shown to transfer well between models trained on the same dataset [23][3]. There are recent attempts trying to diversify the sub-models to make their decisions less redundant. But those strategies fail when the perturbation size of the attack is increased [9].

*This work supported in part by an AFOSR DDDAS grant.

In this paper, we devise an anomaly detection method – instead of trying to robustly classify any given input, we aim to detect if a given input is anomalous. If an input sample is detected, it can either be flagged with a “don’t know” decision or alternative, robust decisionmaking may be invoked for such samples. [14] used class-conditional null distributions to model the DNN’s internal layers (with these null models estimated based on the classifier’s training set). [14] evaluated a novel Kullback-Leibler detection statistic, assessing discrepancy between the DNN’s class decision posterior and a class posterior formed based on the null modeling of internal layer activations. [27, 14] report very good detection performance when adversarial perturbations are small, i.e., for low-confidence attacks. However, these detectors have not been assessed for larger adversarial perturbations (high-confidence attacks).

The development of Generative Adversarial Networks (GANs) gives an alternative (essentially non-parametric) way to model data distributions, which may suffer less model bias than traditional density modeling methods such as Gaussian mixtures. Different GANs models have recently been used for anomaly detection [1, 22]. Given a test image, the GAN’s Discriminator loss and Generator loss are used as detection statistics; the Discriminator loss is just the Discriminator’s output, i.e. the probability that the sample comes from the training distribution. A small probability thus indicates an outlier sample. The Generator loss is the minimum mean squared error (MSE) between Generator-reconstructed images and the test image – anomalous test data tend to incur higher Generator loss [22]. Conventional GANs based detection methods are not very effective because imperceptible perturbations have only weak influence on the Discriminator’s output and the Generator’s reconstruction. Moreover, most GAN-based methods were simply proposed to detect outliers, not TTE attacks.

Defense-GAN [20] is a robust classification method against TTEs. Given a test image, the Generator is used to reconstruct it. The Generator attempts to make *smooth* images; thus, the perturbations of an attack may not be preserved by the Generator’s reconstruction. For class inference, the Generator’s reconstructed image is fed to the Classifier. Experiments demonstrated some effectiveness of this method on datasets such as MNIST and FMNIST. However, Defense-GAN’s performance on CIFAR-10 and ImageNet is poor. A possible reason is that the images for these domains are more complex and variable than for MNIST. Thus, the GAN’s reconstruction of a test image may incur large errors, and may not reproduce features that are critical for accurate classification.

E-ABS [10] has an encoder-decoder model to generate images (i.e., Variational Auto-Encoder - VAE), where the encoder (from input image x to feature vector z) is not class-based and the decoders are class-based (one per class). E-ABS decides to the class with smallest reconstruction loss. They use a discriminator to supervise the VAE so that the latent feature vector z follows the training distribution (it’s unclear how it can be applied to do classification or detection). Conversely, our proposed approach uses a class-conditional discriminator and both the generator and discriminator are used for detection/classification. Also, pure reconstruction based detection methods, e.g., Defense-GAN and f-AnoGAN [21] (cf. next section), don’t have good performance on high-resolution color images such as ImageNet.

In the following, we propose to use a class-conditional GANs model for TTE attack detection.

Our contributions are summarized as follows: (1) We propose an AC-GAN-ADA detector based on an AC-GAN model [18] for anomaly detection of TTEs. (2) We investigate using DNN features from different layers and find (unsurprisingly) that features extracted from layers closer to the DNN’s output are less useful for purpose of detecting TTEs. (3) Our model can correct a DNN’s prediction by providing an alternate prediction based on the class conditional statistics. Thus, our method can be used both for detection and for robust classification. The code of our work will be open-sourced.

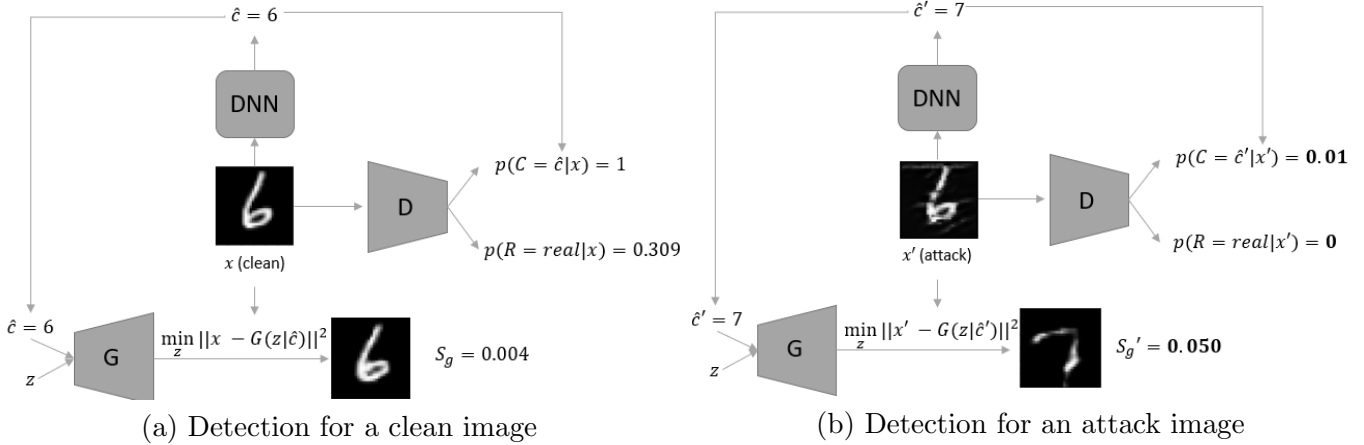


Figure 1: Overview of our AC-GAN-ADA detection method. The conditional distribution is modeled by an AC-GAN model. Block G represents the Generator, D the discriminator, and the DNN is the classifier being attacked. (a) Given a test image x and the DNN’s predicted label \hat{c} , the Generator is used to reconstruct image x conditioned on class \hat{c} by minimizing the Mean Square Error (MSE), where the minimum MSE is the Generator statistic S_g . The outputs of AC-GAN’s Discriminator – $D(x)$, the probability that x follows the training distribution, and a class posterior $\mathbb{P}(C = \hat{c}|x)$ – are two other detection statistics. (b) An example attack image x' gives a higher value for the Generator statistic and lower values for the Discriminator statistics.

2 Background

2.1 Adversarial Examples/Test-Time Evasion Attacks

For image domains, a TTE attacker aims to find a perturbation δ of a correctly classified input image x , yielding $\hat{x} = x + \delta$, such that: (i) by its appearance, \hat{x} still (to a human observer) belongs to the same class as x , but (ii) the Classifier now outputs an incorrect decision $\hat{c}(\hat{x}) \neq \hat{c}(x)$; (iii) The most damaging attacks are *targeted*, wherein the decided class \hat{c} is chosen by the attacker (and thus is not merely a misclassification).

Attack methods can be categorized based on the attacker’s knowledge. In white-box attacks, the attacker has full knowledge of the classifier *and* of any defense mechanism – such attacks could be consistent with an insider threat. In Black-box attacks, the attacker does not have any knowledge of the classifier or of any mounted defense. However, the attacker can query the classifier to learn about it. Here, as commonly considered in previous works [14, 21, 19], we assume a threat model in between these two (black and white box) extremes – the attacker has full knowledge of the classifier, but no knowledge of any defense supporting the classifier.

In the following, we will evaluate defenses against two targeted TTE attacks – the Fast Gradient Sign Method (FGSM) [4] and Carlini-Wagner (CW) [2]. FGSM is a computationally efficient attack method where the perturbation δ is calculated as:

$$\delta = -\varepsilon \cdot \text{sign}(\nabla_x J(x, y_t)). \quad (1)$$

Here ε is the perturbation size, y_t is the target class, and $J(x, y)$ is the loss function given image x and class y . A commonly used loss is the cross entropy loss. CW learns the perturbation based on the following optimization problem:

$$\underset{\delta}{\operatorname{argmax}} \|\delta\|_p + c \cdot f(x + \delta), \quad (2)$$

where $f(x') = \max(\max\{Z(x')_i : i \neq t\} - Z(x')_t, -\kappa)$, t is the target class, and $Z(x')_i$ is the DNN’s output for class i . κ is a hyperparameter which controls the confidence of the attack, and c controls the perturbation size. In our experiments, the L_2 norm was used by the attacker.

2.2 GANs-based Anomaly Detection

In a GANs model, there is a Generator G and a Discriminator D [5]. The Generator transforms a uniform random vector z into a synthetic image $x_g = G(z)$; the Discriminator takes an image x as input and its output $D(x)$ is the probability that x comes from the real (training) distribution. The parameters of the Generator and the Discriminator are learned via a (somewhat complicated) minimax optimization process:

$$\min_G \max_D \mathbb{E}_{x \sim p_{\text{data}}(x)} [\log D(x)] + \mathbb{E}_{z \sim p_w} [\log 1 - D(G(z))]$$

where p_{data} is the training dataset distribution and p_w is typically a uniform distribution. It is shown in [5] that the optimal discriminator output D^* minimizes the Shannon-Jensen metric between p_g and p_{data} so that, given the optimal generator, it cannot discriminate between generated $\sim p_g$ and “real” $\sim p_{\text{data}}$ images, i.e., $p_g \approx p_{\text{data}}$.

For an out-of-distribution image $x \not\sim p_{\text{data}}$, the Discriminator will output a very low posterior. Accordingly, GAN-based methods have been proposed for anomaly detection, e.g., [22, 26, 1, 21]. Generally, GANs-based anomaly detection methods are based on two detection statistics: Generator loss S_g and Discriminator loss S_d [22]:

$$S_g = \min_z \|x - G(z)\|^2, \quad S_d = D(x), \quad (3)$$

where the Discriminator loss is just the posterior probability of a given sample x being generated according to the training distribution ($\sim p_{\text{data}}$). Thus, the smaller the Discriminator loss the more likely the sample is an outlier. The Generator loss is also called the *reconstruction loss*: given a test sample x , we search for a vector z in the Generator’s input space to minimize the reconstruction error $\|x - G(z)\|^2$. A high Generator loss is also indicative of an anomalous sample.

GANs have been used e.g. for detecting lung nodules in lung CT scans or macular degeneration in OCT scans of the retina. However its performance for TTE attack detection is not so good – the perturbations of an attack image are often not detectable by the Discriminator, and do not significantly influence the reconstruction loss. To better exploit GANs for TTE detection, we propose a detector based on *class-conditional* GANs models. We hypothesize that it is easier to learn accurate class-decision conditional GANs models than a single GANs model aiming to well-represent the composite of *all* classes in the problem. This hypothesis will be supported by our experimental results, which show that class-conditional GANs outperform previous GANs approaches and achieve excellent performance in detecting TTE attacks.

There are multiple class-conditional GANs models, e.g., Conditional GAN (cGAN) [15], Auxiliary Classifier GAN (AC-GAN) [18], and cGAN with projection discriminator [16]. In this paper we build our detector around AC-GAN.

2.3 AC-GAN

In AC-GAN, there is a class-conditional Generator, which takes a random vector z and a class label c as input and outputs the synthesized image $x_g = G(z|c)$. Also the Discriminator which, given an input image, gives two outputs: i) $D(x)$, the probability that x comes from the training distribution and ii) $p(c|x)$, the posterior probability that x is from class c . There are two terms in the GANS learning objective – the source loss L_s and the class loss L_c :

$$L_s = \mathbb{E}_{x \sim p_{\text{data}}(x)} [\log \mathbb{P}(R = \text{real}|x)] + \mathbb{E}_{z \sim p_w} [\log \mathbb{P}(R = \text{fake}|G(z))] \quad (4)$$

$$L_c = \mathbb{E}_{x \sim p_{\text{data}}(x)} [\log \mathbb{P}(C = c|x)] + \mathbb{E}_{z \sim p_w} [\log \mathbb{P}(C = c|G(z))] \quad (5)$$

The Discriminator is trained to maximize $L_s + L_c$ while the Generator is trained to minimize $L_s - L_c$.

3 TTE Detection Methodology

	MINST			CIFAR-10		
	CW high conf	CW low conf	FGSM	cw high conf	cw low conf	FGSM
ADA[14]	0.0352	0.0323	0.0367	0.0298	0.0253	0.0305
f-AnoGAN[21]	0.0981	0.0995	0.0887	0.0576	0.0563	0.0566
G-AD	0.1525	0.1517	0.1612	0.0181	0.0254	0.0203
D-AD	0.1915	0.1970	0.1862	0.1881	0.1899	0.1819
All-AD	0.1923	0.1964	0.1905	0.1798	0.1825	0.1618
D-AD-L1	0.1897	0.1873	0.1824	0.1805	0.1787	0.1768

Table 1: pAUC-0.2 results of different detection methods under different attacks.

In our work we consider a class-conditional version of the anomaly detection method in [22]. In AC-GAN we have three test statistics. Given an input image x and the DNN-predicted class \hat{c} , these test statistics are:

$$S_R = D(x) \quad (6)$$

$$S_C = p(C = \hat{c}|x) \quad (7)$$

$$S_g = \min_z \|x - G(z|\hat{c})\|^2 \quad (8)$$

S_R and S_C are the outputs of the Discriminator, and S_g is the Generator’s class-conditional reconstruction loss. An illustration of our detection inference is shown in Fig. 1.

3.1 Detection methods

A single discriminator test statistic S_d can be obtained by aggregating S_R and S_C based on an independence assumption for these two probabilities, i.e. via:

$$S_d = \log(D(x)) + \log(p(C = \hat{c}|x)). \quad (9)$$

This is called Discriminator based Anomaly Detection (D-AD). The first (class-independent) term in S_d penalizes images with large perturbation size, while the second term penalizes images with low probability for the class to which the DNN is deciding.

Under Generator based Anomaly Detection (G-AD), the Generator statistic S_g is solely used to detect anomalous images. Again, out-of-distribution image-label pairs will give larger values of S_g .

We can also combine all the test statistics to make a detection. For example, define the vector $S = [S_R, S_C]$. One can model S using e.g. a Gaussian mixture model (GMM), with anomalies then detected based on a p-value assessed with respect to the GMM. We denote this method as All-AD.

3.2 Detecting based on internal layer features

Recall that previous Anomaly Detection methods, e.g., [27, 14, 19] detect anomalies based on internal layer DNN features. They model the null distribution for these features using Gaussian mixture models, kernel density estimation or K-nearest neighbors (KNN), respectively. As we discussed above, the AC-GAN model can also capture the conditional null distribution of the internal layer features. Consider an L -layer DNN h (e.g., of the ResNet type). For a test image x with predicted class $\hat{c} = h_L(x)$, we first extract a feature vector from the k^{th} DNN layer, $h_k(x)$, which is modeled by an AC-GAN. Then the detection statistics discussed in Eq. (6) - Eq. (8) can be used just by replacing $x = h_0(x)$ by $h_k(x)$.

3.3 Robust Classification

Based on the class conditional detection statistics of the Generator and the Discriminator, beyond detecting attacks we can also *correct* the Classifier’s prediction. The Discriminator captures the class conditional distribution of the input data, so the class under which the input image is least *atypical* can be predicted as the correct class. We use the Discriminator’s maximum *a posteriori* class ($c_D = \arg \max_i p(C = i|x)$) as the corrected class decision in our experiments.

4 Experiments

We evaluated the performance of our AC-GAN based Anomaly detection methods on two well-known image classification datasets: MNIST [12] and CIFAR-10 [11]. The ResNet-18 [7] model is used as the DNN classifier model. CW attack and FGSM attack are used as two adversarial attack methods. We used different AC-GAN structures for the MNIST and CIFAR-10 datasets.

4.1 Performance of Anomaly Detection

For anomaly detection, we now report the results of the proposed D-AD, G-AD and All-AD methods. D-AD-L1 means the features extracted from the first convolutional layer are used to do detection. For all other variants of our method (D-AD, G-AD, and All-AD) the GANs is modeling the input (image). ADA [14] is used as a Class-based Anomaly Detection baseline. F-anoGAN [21] is used as a GAN based anomaly detection baseline. We implemented or replicated all the methods mentioned above. For the targeted CW attack (2) , we set the model parameter $\kappa = 14$ (which is a common setting) and searched for the minimum value of c to make successful high-confidence and low-confidence attacks. For high-confidence attacks, we perturbed the image so that the DNN’s output target class posterior is larger than 90%. For low-confidence attacks, we make perturbations until the target class posterior is larger than that for any other class.

For the FGSM attack (1), we chose $\varepsilon = 0.3$ and only retained the successfully (targeted) attacked images. We evaluated performances of all the anomaly detection methods using the partial area under the ROC curve for FPR below 0.2 (pAUC-0.2). pAUC was used assessed because the most practically important detection performance is in the low false-positive regime. The results are shown in Table 1. We can see our methods, which combine class decision conditioned anomaly detection and GAN based anomaly detection, outperform both the non-conditional GAN based anomaly detection method and the class-conditional ADA method. We can see from the table that the best-performing versions of our method either use both the discriminator and generator statistics (ALL-AD) or just use the discriminator (D-AD) – the generator is modestly helpful for MNIST, but unhelpful for CIFAR-10. Note also the large performance gains of our method compared to the ADA and f-AnoGAN baselines, for both data sets, and under all attacks – the baseline methods give unacceptably low pAUC detection power.

	MINST		CIFAR-10	
	CW-HC	CW-LC	CW-HC	CW-LC
D-GAN[20]	0.9247	0.9273	0.2089	0.2079
RC-Image	0.8951	0.8816	0.8266	0.8191
RC-Layer1	0.8295	0.8204	0.7643	0.7420

Table 2: Robust classification accuracy. CW-HC means CW high confidence attack, CW-LC means CW low confidence attack. D-GAN means Defense-GAN method.

4.2 Performance of Robust Classification

In Table 2, we present the results of our robust classification method described in Section 3.3. For Robust Classification Image (RC-Image) method, we perform the classification using images as input. For the

Robust Classification Layer1 (RC-L1), the features extracted from the first convolutional layer of the DNN are used for classification. We compare our methods with the Defense-GAN baseline. We can see from Table 2 that the performance of Defense-GAN is better than our methods on MNIST dataset, but our methods greatly outperform Defense-GAN on CIFAR-10.

4.3 Visualizing the distribution of internal layer features

The AC-GAN framework can model the distribution of clean images (inputs to the DNN) or of internal layer features (Section 3.2). It is useful to visualize these layers, in order to help understand how effective a given layer is for discriminating between attack and clean images. At test time, when an image or internal layer feature is fed into the Discriminator, we just extract the penultimate layer’s output of the discriminator, and visualize the outputs using t-SNE [25], which is a t-distributed stochastic neighbor embedding method used for nonlinear dimension reduction. The visualization results are shown in Figure 2. Consider in particular images perturbed from class ‘0’ to class ‘1’ (orange triangle points). In the input layer, clean 0, clean 1, and attack 0 are well-separated from each other. In internal layer 1, attacked class 0 images still follow the clean ‘0’ distribution (and hence are discriminable from clean ‘1’); the internal layer 2 features, for attacked images, fall in between clean ‘0’ and clean ‘1’; the penultimate layer DNN features are very close to some clean ‘1’ samples, which is indicative that these features cannot reliably discriminate between clean and attacked images.

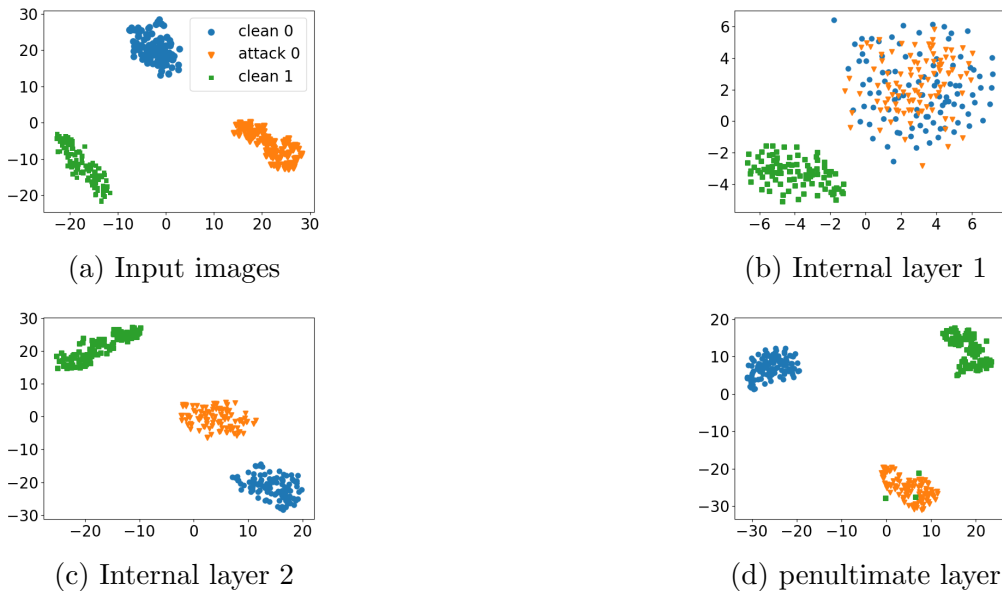


Figure 2: Visualization of features from different DNN (ResNet) layers using the t-SNE method on the MNIST dataset. The features visualized in each sub-figures are from: (a) the input layer (images), (b) the first convolutional layer, (c) the 10th convolutional layer, or (d) the penultimate layer. The blue circle points are clean images from class ‘0’, the green rectangle points are clean images from class ‘1’, the orange triangle points are attack images which are perturbed from class ‘0’ to class ‘1’.

5 Conclusions

In this paper, we proposed an AC-GAN based Anomaly detection method to detect TTE attacks. We empirically showed that our method achieves state-of-the-art performance on two benchmark datasets, considering both low and high confidence attacks. Our method can also be used to perform robust classification. Our results indicate that, generally, internal-layer activations close to the input are more useful in detecting both high and low confidence TTEs, compared with activations closer to the output layer. In future work, other GANs models may be investigated e.g., [16].

References

- [1] Samet Akcay, Amir Atapour-Abarghouei, and Toby P Breckon. GANomaly: Semi-supervised anomaly detection via adversarial training. In *Asian Conference on Computer Vision*, pages 622–637. Springer, 2018.
- [2] Nicholas Carlini and David Wagner. Towards evaluating the robustness of neural networks. In *IEEE Symposium on Security and Privacy*, pages 39–57. IEEE, 2017.
- [3] Ambra Demontis, Marco Melis, Maura Pintor, Matthew Jagielski, Battista Biggio, Alina Oprea, Cristina Nita-Rotaru, and Fabio Roli. Why do adversarial attacks transfer? Explaining transferability of evasion and poisoning attacks. In *28th USENIX Security Symposium*, pages 321–338, 2019.
- [4] I. Goodfellow, J. Shlens, and C. Szegedy. Explaining and harnessing adversarial examples. In *Proc. ICLR*, 2015.
- [5] J. Goodfellow, J. Pouget-Abadie, M. Mirza, B. Xu, D. Warde-Farley, S. Ozair, A. Courville, and Y. Bengio. Generative adversarial networks. In *Proc. Neural Information Processing Systems (NIPS)*, 2014.
- [6] Lars Kai Hansen and Peter Salamon. Neural network ensembles. *IEEE Transactions on Pattern Analysis and Machine Intelligence*, 12(10):993–1001, 1990.
- [7] Kaiming He, Xiangyu Zhang, Shaoqing Ren, and Jian Sun. Deep residual learning for image recognition. In *Proceedings of the IEEE Conference on Computer Vision and Pattern Recognition*, pages 770–778, 2016.
- [8] Dan Hendrycks and Kevin Gimpel. A baseline for detecting misclassified and out-of-distribution examples in neural networks. *arXiv preprint arXiv:1610.02136*, 2016.
- [9] Andrew Ilyas, Shibani Santurkar, Dimitris Tsipras, Logan Engstrom, Brandon Tran, and Aleksander Madry. Adversarial examples are not bugs, they are features. *arXiv preprint arXiv:1905.02175*, 2019.
- [10] An Ju and David Wagner. E-ABS: Extending the Analysis-By-Synthesis Robust Classification Model to More Complex Image Domains. In *Proc. AISEc*, Nov. 2020.
- [11] Alex Krizhevsky. Learning multiple layers of features from tiny images. <http://www.cs.toronto.edu/~kriz/learning-features-2009-TR.pdf>, 2009.
- [12] Yann LeCun and Corinna Cortes. MNIST handwritten digit database. 2010.
- [13] Aleksander Madry, Aleksandar Makelov, Ludwig Schmidt, Dimitris Tsipras, and Adrian Vladu. Towards deep learning models resistant to adversarial attacks. *arXiv preprint arXiv:1706.06083*, 2017.
- [14] David Miller, Yujia Wang, and George Kesidis. When not to classify: Anomaly detection of attacks (ADA) on DNN classifiers at test time. *Neural Computation*, 31(8):1624–1670, 2019.
- [15] Mehdi Mirza and Simon Osindero. Conditional generative adversarial nets. *arXiv preprint arXiv:1411.1784*, 2014.
- [16] Takeru Miyato and Masanori Koyama. cGANs with projection discriminator. *arXiv preprint arXiv:1802.05637*, 2018.

- [17] Anh Nguyen, Jason Yosinski, and Jeff Clune. Deep neural networks are easily fooled: High confidence predictions for unrecognizable images. In *Proceedings of the IEEE Conference on Computer Vision and Pattern Recognition*, pages 427–436, 2015.
- [18] Augustus Odena, Christopher Olah, and Jonathon Shlens. Conditional image synthesis with auxiliary classifier GANs. In *International Conference on Machine Learning*, pages 2642–2651. PMLR, 2017.
- [19] Jayaram Raghuram, Varun Chandrasekaran, Somesh Jha, and Suman Banerjee. Detecting Anomalous Inputs to DNN Classifiers By Joint Statistical Testing at the Layers. *arXiv preprint arXiv:2007.15147*, 2020.
- [20] Pouya Samangouei, Maya Kabkab, and Rama Chellappa. Defense-GAN: Protecting classifiers against adversarial attacks using generative models. *arXiv preprint arXiv:1805.06605*, 2018.
- [21] Thomas Schlegl, Philipp Seeböck, Sebastian M Waldstein, Georg Langs, and Ursula Schmidt-Erfurth. f-AnoGAN: Fast unsupervised anomaly detection with generative adversarial networks. *Medical Image Analysis*, 54:30–44, 2019.
- [22] Thomas Schlegl, Philipp Seeböck, Sebastian M Waldstein, Ursula Schmidt-Erfurth, and Georg Langs. Unsupervised anomaly detection with generative adversarial networks to guide marker discovery. In *International Conference on Information Processing in Medical Imaging*, pages 146–157. Springer, 2017.
- [23] Florian Tramèr, Alexey Kurakin, Nicolas Papernot, Ian Goodfellow, Dan Boneh, and Patrick McDaniel. Ensemble adversarial training: Attacks and defenses. *arXiv preprint arXiv:1705.07204*, 2017.
- [24] Dimitris Tsipras, Shibani Santurkar, Logan Engstrom, Alexander Turner, and Aleksander Madry. Robustness may be at odds with accuracy. *arXiv preprint arXiv:1805.12152*, 2018.
- [25] Laurens Van der Maaten and Geoffrey Hinton. Visualizing data using t-SNE. *Journal of Machine Learning Research*, 9(11), 2008.
- [26] Houssam Zenati, Chuan Sheng Foo, Bruno Lecouat, Gaurav Manek, and Vijay Ramaseshan Chandrasekhar. Efficient GAN-based anomaly detection. *arXiv preprint arXiv:1802.06222*, 2018.
- [27] Zhihao Zheng and Pengyu Hong. Robust detection of adversarial attacks by modeling the intrinsic properties of deep neural networks. In *Proceedings of the 32nd International Conference on Neural Information Processing Systems*, pages 7924–7933, 2018.